AAC Journals.ASM.org

Bactericidal Activity of Ceragenin CSA-13 in Cell Culture and in an Animal Model of Peritoneal Infection

Robert Bucki,[a,b,c] Katarzyna Niemirowicz,[a] Urszula Wnorowska,[a] Fitzroy J. Byfield,[c] Ewelina Piktel,[a] Marzena Wątek,[d] Paul A. Janmey,[c] Paul B. Savage[e]

Department of Microbiological and Nanobiomedical Engineering, Medical University of Bialystok, Bialystok, Poland[a]; Department of Physiology, Pathophysiology, and Microbiology of Infections, Faculty of Health Sciences, Jan Kochanowski University in Kielce, Kielce, Poland[b]; University of Pennsylvania, Institute for Medicine and Engineering, Roy and Diana Vagelos Research Laboratories, Philadelphia, Pennsylvania, USA[c]; Department of Hematology, Holy Cross Oncology Center, Kielce, Poland[d]; Department of Chemistry and Biochemistry, Brigham Young University, Provo, Utah, USA[e]

Ceragenins constitute a novel family of cationic antibiotics characterized by a broad spectrum of antimicrobial activities, which have mostly been assessed *in vitro*. Using a polarized human lung epithelial cell culture system, we evaluated the antibacterial activities of the ceragenin CSA-13 against two strains of *Pseudomonas aeruginosa* (PAO1 and Xen5). Additionally, the biodistribution and bactericidal activity of a CSA-13–IRDye 800CW derivate were assessed using an animal model of peritoneal infection after PAO1 challenge. In cell culture, CSA-13 bactericidal activities against PAO1 and Xen5 were higher than the activities of the human cathelicidin peptide LL-37. Increased CSA-13 activity was observed in polarized human lung epithelial cell cultures subjected to butyric acid treatment, which is known to increase endogenous LL-37 production. Eight hours after intravenous or intraperitoneal injection, the greatest CSA-13–IRDye 800CW accumulation was observed in mouse liver and kidneys. CSA-13–IRDye 800CW administration resulted in decreased bacterial outgrowth from abdominal fluid collected from animals subjected to intraperitoneal PAO1 infection. These observations indicate that CSA-13 may synergistically interact with antibacterial factors that are naturally present at mucosal surfaces and it maintains its antibacterial activity in the infected abdominal cavity. Cationic lipids such as CSA-13 represent excellent candidates for the development of new antibacterial compounds.

Ceragenins, synthetic cationic steroids, represent a new class of antimicrobial agents designed to mimic the activities of natural cationic antibacterial peptides (CAPs) (1, 2). They are characterized by a broad spectrum of bactericidal activities against viruses, Gram-negative and Gram-positive bacteria (3–5), fungi, and parasites (6). Like that of natural CAPs, the bactericidal activity of ceragenins declines in the presence of blood plasma; the development of ceragenins is currently directed to topical applications (7–9). Due to its high antibacterial activity, CSA-13 is the most promising ceragenin. A recent finding showed that CSA-13 retained potent antibacterial activity over the course of 30 serial passages, indicating that bacteria are very unlikely to develop resistance against this compound (10). In addition to bactericidal activity against planktonic bacteria, CSA-13 disintegrates bacterial biofilms in a very efficient manner, at a concentration slightly higher than that required for bactericidal activity against planktonic bacteria (11, 12). In cell culture models, treatment with CSA-13 was found to suppress HCT116 colon cancer cell proliferation and to increase apoptosis and was associated with cell cycle arrest at the G_1/S phase (13). All cellular activities of CSA-13 involve interactions with plasma membranes, and the mechanism of bacterial cell killing is associated with changes in membrane organization after CSA-13 insertion into the plasma membrane, which results in membrane depolarization (14, 15).

The epithelium plays a predominant role in innate resistance to pathogen infections by providing a mechanical barrier to microbial entry, signaling different immunocompetent cells, and directing the killing of bacteria (16). Consistent with the ability of isolated epithelial cells to kill bacteria, various antibacterial agents that are released from epithelial cells and leukocytes have been characterized (17, 18). Among those agents, antibacterial human β-defensins 1 and 2 and LL-37 peptide, which is derived from human cathelicidin (hCAP-18), are key factors preventing pathogen invasion and ensuring the effective eradication of pathogens (19, 20). Production of CAPs, including LL-37, by epithelial cells can be activated by vitamin D_3, butyric acid, and retinoic acid (21, 22). The development of new antibacterial agents requires evaluation of their activities in different settings, including animal models (23). Peritonitis after direct administration of bacteria mimics the abdominal cavity infections that develop after incidents of digestive tract perforation or in patients undergoing peritoneal dialysis (24). In this study, we observed strong bactericidal and anti-inflammatory activities of CSA-13 in a cell culture system mimicking the airway epithelium and in a mouse model of peritoneal infection. These findings suggest a strong potential of CSA-13 for future development as a new antibiotic.

MATERIALS AND METHODS

Materials. LL-37 peptide (LLGDFFRKSKEKIGKEFKRIVQRIKDFLRNL VPRTES) was purchased from Peptide 2.0 (Chantilly, VA). Sodium butyrate, lipopolysaccharide (LPS) from *Pseudomonas aeruginosa* serotype 10, and cetrimide-containing agar were purchased from Sigma. *P. aerugi-*

Received 14 March 2015 Returned for modification 25 May 2015
Accepted 20 July 2015

Accepted manuscript posted online 27 July 2015

Citation Bucki R, Niemirowicz K, Wnorowska U, Byfield FJ, Piktel E, Wątek M, Janmey PA, Savage PB. 2015. Bactericidal activity of ceragenin CSA-13 in cell culture and in an animal model of peritoneal infection. Antimicrob Agents Chemother 59:6274–6282. doi:10.1128/AAC.00653-15.

Address correspondence to Robert Bucki, buckirobert@gmail.com.

doi:10.1128/AAC.00653-15

nosa Xen5, engineered through conjugation and transposition of a plasmid carrying transposon Tn*5 luxCDABE*, was purchased from Caliper Life Sciences. Luria-Bertani (LB) broth and tryptic soy broth (TSB) were purchased from Difco (Sparks, MD). Anti-hCAP-18/LL-37 antibody was obtained from Novus Biologicals (Littleton, CO). The lactate dehydrogenase (LDH) cytotoxicity assay kit was obtained from BioVision (Mountain View, CA), and IRDye 800CW was from Li-Cor (Polygen, Wroclaw, Poland).

Cell culture. Primary normal human bronchial epithelial (NHBE) cells (Lonza, Walkersville, MD) were cultured in T-75 flasks with bronchial epithelial growth medium (BEGM) containing all supplements (bovine pituitary extract, hydrocortisone, human epidermal growth factor, epinephrine, transferrin, insulin, retinoic acid, triiodothyronine, and final concentrations of 30 μg/ml gentamicin and 15 ng/ml amphotericin [GA-1000]). Cells were allowed to grow until 90% confluent. Cells were then trypsinized and seeded at a density of $\sim 4 \times 10^5$ cells/ml, in differentiation medium (BEGM without triiodothyronine, supplemented with butyric acid), on 0.4-μm-pore membrane inserts coated with a 3:1 mixture of bovine collagen I and human fibronectin. After the cells had reached confluence, when transepithelial resistance was $>500\ \Omega \cdot cm^2$, the differentiation medium was removed from the apical surface of the cells and the cells were allowed to grow at the air-liquid interface until polarized epithelial cell monolayers developed, as assessed by mucin production (staining with Texas Red-conjugated *Ulex europaeus* agglutinin; Sigma, St. Louis, MO) and the presence of cilia (expression of α-tubulin). Human lung epithelial carcinoma cells (line A549) were cultured at 37°C in Dulbecco's modified Eagle's medium (DMEM) (BioWhittaker, Walkersville, MD) supplemented with 10% fetal bovine serum (HyClone, Logan, UT), in 5% CO_2. To evaluate CSA-13 and LL-37 antibacterial activities for all cell types, growth medium was changed to DMEM and a *P. aeruginosa* suspension was added to the apical surface of cell monolayers, followed by the addition of antibacterial agents.

Bactericidal activity in a cell culture setting. *P. aeruginosa* cells grown to mid-log phase at 37°C (controlled by evaluation of the optical density at 600 nm [OD_{600}]) were resuspended in DMEM. CSA-13 and LL-37 bactericidal activities were evaluated using a bacterial killing assay. After standard incubations of bacteria with different concentrations of antibacterial agents at 37°C, samples were placed on ice and diluted 10- to 1,000-fold, and 10-μl aliquots of each dilution were spotted on cetrimide-containing agar. The numbers of colonies for each dilution were counted the following morning. The CFU per milliliter for the individual samples were determined from the dilution factor.

F-actin, α-tubulin, and hCAP-18/LL-37 staining. Cells treated with various reagents or untreated confluent monolayers of human lung polarized epithelial cells were washed three times with phosphate-buffered saline (PBS) and fixed for 10 min at room temperature (RT) with 4% paraformaldehyde (Sigma-Aldrich), followed by an additional rinse with PBS. Cells were then permeabilized for 5 min at RT with 0.1% Triton X-100. For localization and structure analysis of F-actin, cells were stained for 30 min with a 1:100 solution of rhodamine-labeled phalloidin (Invitrogen) in PBS. For NHBE, the polarized monolayer was first stained with 3 μg/ml antitubulin monoclonal antibody (Amersham, Arlington Heights, IL). Assessment of hCAP-18/LL-37 peptide expression in control and A549 polarized lung epithelial cells treated with butyric acid was performed using immunostaining after fixation. The immunostaining was performed after 48 h of treatment with 1 or 4 mM sodium butyrate. Under all conditions, A549 cells were subjected to permeabilization with Triton X-100 before the addition of anti-hCAP-18/LL-37. Sodium butyrate was shown previously to induce hCAP-18/LL-37 expression in the human colorectal cancer cell line Caco-2 (25, 26). Fluorescence was assessed using an inverted research microscope (Leica DM IRBE system).

Evaluation of cytotoxicity toward lung epithelial cells. Epithelial cell cytotoxicity associated with bacterial infection was assessed by measurements of LDH released into the culture supernatants, which were compared with the total enzyme activity recovered from lung epithelial cell monolayers after cell lysis with 0.1% Triton X-100. An LDH colorimetric assay kit was used according to the manufacturer's instructions.

Bioelectrical measurements. The transmonolayer electrical resistance was measured using an EVOM volt-ohm meter (World Precision Instruments, Berlin, Germany) equipped with a pair of STX-2 chopstick electrodes. Electrodes were placed in the upper and lower chambers, and resistance was measured with the volt-ohm meter.

CSA-13 labeling with IRDye 800CW. The labeling of CSA-13 with IRDye 800CW was performed according to a previously used procedure (27). CSA-13 was suspended in phosphate buffer at pH 7.4. At this pH, the N-terminal ceragenin groups react with the *N*-hydroxysuccinimide (NHS) ester to form stable covalent amide bonds. The efficiency of labeling was nearly 90%.

Antimicrobial testing of CSA-13–IRDye 800CW *in vitro*. The bactericidal activities of CSA-13, CSA-13 labeled with dye, and IRDye 800CW were measured using a killing assay. Briefly, to perform the killing assay, *P. aeruginosa* PAO1 was grown to mid-log phase at 37°C, resuspended in PBS, and brought to 10^8 CFU/ml. The cells were then diluted in PBS containing different concentrations of CSA-13, CSA-13 labeled with dye, or IRDye 800CW. After 1 h of incubation at 37°C, the plates were transferred to ice and the suspensions were diluted 10- to 1,000-fold in PBS. Then, 10-μl aliquots were spotted on cetrimide-containing agar plates for overnight culture at 37°C, after which CFU were determined. *P. aeruginosa* PAO1 biofilms were grown for 48 h at 37°C, with and without antibacterial agents, in 96-well microtiter plates. Each well was washed four times with deionized water to remove planktonic bacteria. Biofilm mass was evaluated using crystal violet (0.1%) staining. Excess stain was rinsed off with deionized water, and plates were dried. Then, 100 μl ethanol was added, and the optical density (OD) was determined at 570 nm. These OD values were considered measurements of bacteria adhering to the surface and forming a biofilm. A killing assay was performed to assess the activity of CSA-13 labeled with IRDye 800CW in peritoneal fluid. Briefly, *P. aeruginosa* PAO1 was grown to mid-log phase at 37°C, resuspended in PBS, and brought to $\sim 10^8$ CFU/ml. Bacteria were then diluted in PBS mixed with 50% human peritoneal fluid containing different concentrations of CSA-13 labeled with IRDye 800CW. After 1 h of incubation at 37°C, the plates were transferred to ice and the suspensions were diluted 10- to 1,000-fold in PBS. Then, 10-μl aliquots were spotted on cetrimide-containing agar plates for overnight culture at 37°C, after which CFU were determined.

Biodistribution of CSA-13–IRDye 800CW and bactericidal activity *in vivo*. A 100-μl volume of CSA-13 covalently labeled with the fluorescent dye IRDye 800CW was injected intravenously ($n = 5$) or intraperitoneally (i.p.) ($n = 5$) into 10-week-old nude female mice (strain Cby.Cg.Foxn1nu/cmdb). At predetermined times (0.5, 4, and 8 h postinjection), animals were anesthetized with isoflurane and whole-body scans were performed. After the last time point, a lethal injection of xylazine-ketamine was administered, and then the brain, heart, lungs, liver, pancreas, spleen, kidneys, and bladder were isolated. The fluorescence of isolated organs was recorded in the 800-nm channel using an Odyssey imaging system. Pharmacokinetic parameters, including maximum plasma concentration (C_{max}), time to reach C_{max} (T_{max}), biological half-life ($t_{1/2}$), total area under the concentration-time curve (AUC_{total}), mean residence time (MRT), and clearance (CL), were calculated using Kinetica 5.0 software. The binding of the ceragenin to plasma proteins was assessed spectrophotometrically. The concentrations of CSA-13 in ultrafiltrates were determined by measuring the absorbance at 230 nm (A_{230}) in a spectrophotometer, compared with drug-free ultrafiltrate as a blank (28). To evaluate antibacterial activity, mice were infected intraperitoneally with 100 μl of PAO1 bacteria suspended in LB broth at an OD_{600} of 0.1, which corresponds to 6×10^6 CFU. Two hours after infection, a treated group received 5 μg/g CSA-13–IRDye 800CW injected i.p. ($n = 5$) and a control group received 0.9% NaCl ($n = 5$). At 10 h postinfection, a lethal injection of xylazine-ketamine was administered. Blood was collected into EDTA-containing tubes (1% solution) by cardiac puncture. After serial

dilution, peritoneal fluid was spotted on cetrimide-containing agar plates for overnight culture to determine bacterial outgrowth. Additionally, the spleens were removed and changes in weight (possibly due to inflammation) were assessed.

Statistical analysis. Data are reported as the mean ± standard deviation (SD) of three to six experiments. Data analysis was performed using one-way analysis of variance (ANOVA) with a *post hoc* Bonferroni analysis test.

RESULTS

CSA-13 treatment prevents morphological changes of human polarized lung epithelial cells occurring after bacterial infections. When subjected to *P. aeruginosa* Xen5 infection (with the addition of bacteria to the apical surface), confluent (as indicated by transepithelial resistance of $>500\ \Omega \cdot cm^2$) and fully differentiated, polarized, primary human lung epithelial cells (Fig. 1A) showed reduced cell-cell junctions (appearance of large gaps), decreased expression of α-tubulin (decreased numbers of cells with cilia), and increased cortical F-actin (Fig. 1B). These changes were less pronounced in samples to which CSA-13 had been added following bacterial inoculation (Fig. 1C and D). Epithelial cell damage associated with the presence of bacteria was indicated by increased LDH activity (78% higher than that detected in control samples at the 18-h time point), which was prevented by CSA-13 addition, as indicated by decreases in LDH activity to 67 and 51% after treatment with 10 and 30 μM, respectively (data not shown).

Bactericidal activity of CSA-13 in a cell culture system is greater than that of the cathelicidin LL-37. As indicated by the data in Fig. 1E, the addition of CSA-13 (10 μM) to the apical surface of primary lung epithelial cells infected with *P. aeruginosa* Xen5 resulted in rapid killing (no bacterial outgrowth from the apical surface was observed during the period between 30 min and 6 h). Since the presence of mucin at the surface of primary lung epithelial cells might have affected the precise collection of samples for bacterial growth assays, we also assessed the presence of *P. aeruginosa* Xen5 by monitoring changes in bacterial luminescence (Fig. 1F). According to the *in vitro P. aeruginosa* Xen5 growth curve, 2×10^6 mean photons/s corresponds to an OD_{600} of 0.5, which translates to $\sim 10^8$ CFU/ml. At 6 h after the addition of 10 or 30 μM CSA-13 to infected cultures, luminescence was decreased by 89 or 97%, respectively. Since luminescence measurements may collect signals from bacteria that are trapped in mucin or have bound to or have migrated inside the epithelial cells (29, 30), differences between bacterial outgrowth and luminescence signals might be observed (Fig. 1E and F). Indeed, no bacterial outgrowth from the apical surface of cultured cells was observed when limited luminescence was recorded (Fig. 1E and F). The changes in *P. aeruginosa* Xen5 chemiluminescence at various time points after treatment with CSA-13 or LL-37 are shown in Fig. 1F. In our cell culture system, bacterial killing and decreased bacterial luminescence after the addition of CSA-13 were greater than the effects of LL-37.

Sodium butyrate increases antibacterial activities of CSA-13 and LL-37 in a cell culture system. The intensity of *P. aeruginosa* Xen5 luminescence in wells containing confluent cultures of bacteria-infected A549 lung epithelial cells decreased 1, 2, and 8 h after CSA-13 addition (Fig. 1G to I). The observed decreases depended on the CSA-13 concentration and the incubation time (Fig. 1J and K). The antibacterial effects of CSA-13 and LL-37 were much greater in samples treated with butyric acid, which was shown previously to increase hCAP-18 expression (21, 22). Indeed, immunostaining of A549 cells with anti-hCAP-18/LL-37 antibody after treatment with retinoic acid or butyric acid indicated greater expression of hCAP-18 in treated cells, compared to untreated cells (data not shown).

CSA-13 and LL-37 decrease IL-8 release in polarized A549 cells infected with *P. aeruginosa* Xen5. Interleukin-8 (IL-8) concentrations in cell culture medium collected from the lower chamber of polarized A549 cultures are shown in Fig. 1L. Approximately 40% decreases in IL-8 released from cells grown in the presence of sodium butyrate were observed in samples treated with 30 μM CSA-13 or 30 μM LL-37.

CSA-13–IRDye 800CW synthesis and bodily distribution in a mouse model of peritoneal infection. The overall synthesis procedure for CSA-13 labeled with fluorescent dye (IRDye 800CW) is shown in Fig. 2a. The CSA-13–IRDye 800CW fluorescent product was obtained via *N*-hydroxysuccinimide (NHS) ester-mediated derivatization, which involves reaction of the NHS group with the primary amine of the ceragenin CSA-13. The conjugation reaction is performed under physiological conditions (pH 7.4) at room temperature and results in an amide bond linkage. The reaction of NHS esters with primary amines is fast, and cross-linking with this reaction is widely utilized in pharmacokinetic studies of bioactive compounds. *In vivo* imaging of ceragenin biodistribution in whole mice is shown in Fig. 2b. Eight hours after intravenous or intraperitoneal injection, the highest levels of CSA-13–IRDye 800CW accumulation were observed in liver and kidneys. However, higher levels of accumulation were detected in liver and bladder after intravenous injection, compared to intraperitoneal administration (Fig. 2c). Nonsignificant differences in CSA-13–IRDye 800CW organ distribution in healthy versus infected mice were observed (Fig. 2d). Various pharmacokinetic parameters, including total area under the concentration-time curve (AUC_{total}), maximum plasma concentration (C_{max}), time to reach C_{max} (T_{max}), biological half-life ($t_{1/2}$), mean residence time (MRT), and clearance (CL) of the ceragenin, were calculated through reconstruction of the fluorescence signals. The protein binding of the ceragenin was determined by ultrafiltration of whole plasma containing CSA-13 (2%) and measurement of the A_{230} of free (unbound) compound in the resulting ultrafiltrate. The basic pharmacokinetic parameters of CSA-13 are summarized in Table 1.

CSA-13–IRDye 800CW exerts antibacterial activity in a mouse model of peritoneal infection. Figure 3A shows that functionalization of CSA-13 by attachment of IRDye 800CW did not affect CSA-13 antibacterial activity against the planktonic form of *P. aeruginosa*. Both free CSA-13 and its labeled derivative CSA-13–IRDye 800CW were able to prevent bacterial growth at a concentration of 2 μg/ml (IRDye 800CW lacks intrinsic bactericidal activity). In addition to bactericidal activity against planktonic PAO1 bacteria, CSA-13 and CSA-13–IRDye 800CW were able to prevent biofilm formation and to kill bacteria embedded in the biofilm matrix. As indicated in Fig. 3, biofilm mass formed in the presence of 10 μg/ml CSA-13–IRDye 800CW was reduced more than 90%. To imitate *in vivo* conditions and to select a dose of CSA-13–IRDye 800CW for an animal model of peritoneal infection, the bactericidal activity of CSA-13–IRDye 800CW was assessed in a PBS-human ascites (1:1) mixture. As shown in Fig. 3C, at a concentration of 5 μg/ml, CSA-13–IRDye 800CW exerted strong bactericidal activity against the PAO1 strain ($OD_{600} = 0.1$). Bactericidal activity of CSA-13–IRDye 800CW was also observed in a mouse model of peritoneal infection. Six-week-old nude mice

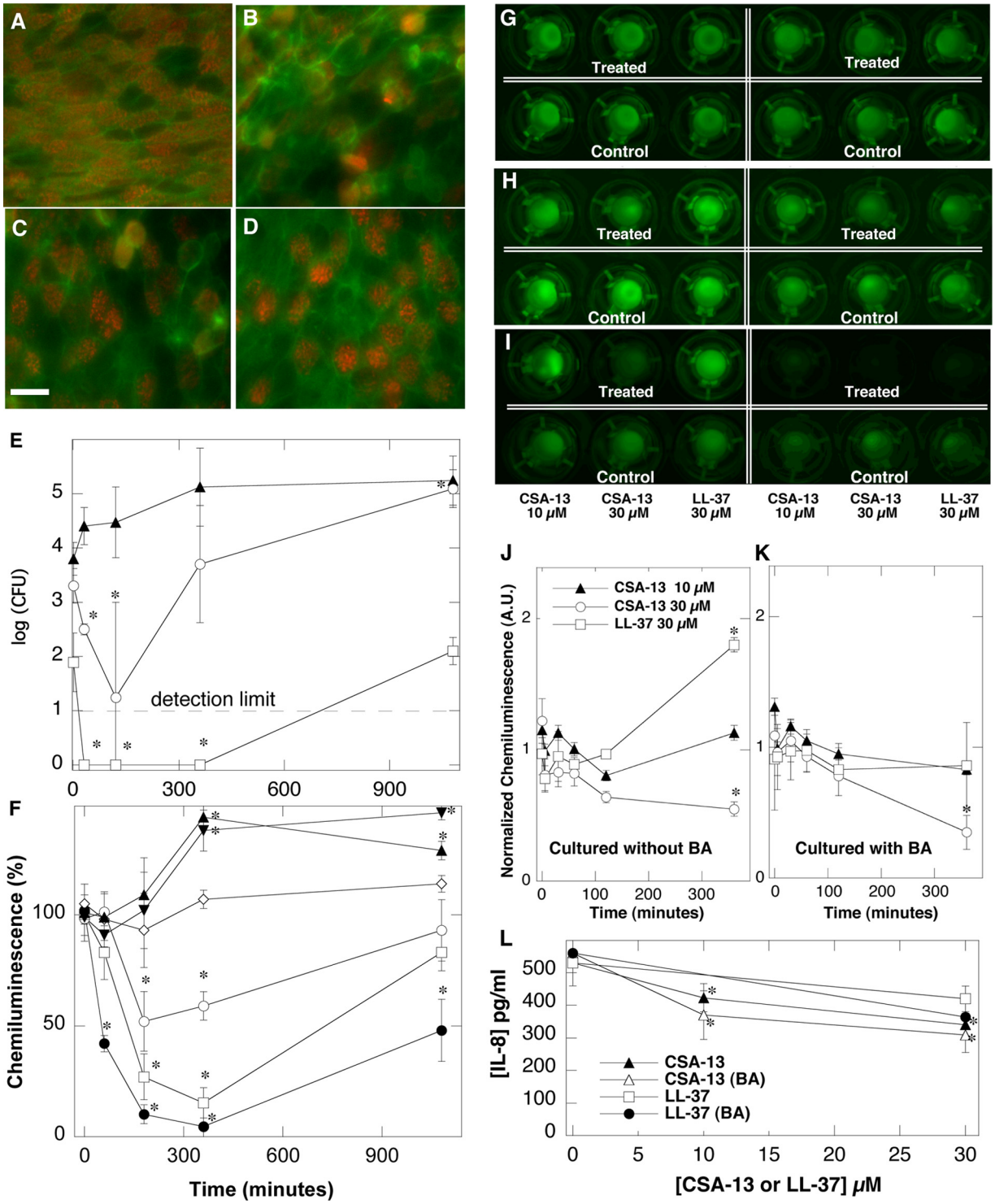

FIG 1 (A to D) Morphology of human bronchial epithelial cells (5-week polarized cultures grown on 0.4-μm-pore inserts) subjected to *P. aeruginosa* Xen5 infection and treatment with the ceragenin CSA-13. The scale bar represents 15 μm. (A) Control epithelial cells. (B) Infected epithelial cells. (C and D) Infected epithelial cells treated with 10 μM CSA-13 (C) or 30 μM CSA-13 (D) 18 h after the addition of bacteria. Green staining, F-actin; red staining, α-tubulin (cilia). (E and F) *P. aeruginosa* Xen5 outgrowth (E) and chemiluminescence (F) from the apical interface of human bronchial epithelial cells at different times. ▲, 2 μM LL-37; ▼, 10 μM LL-37; ◇, 30 μM LL-37; ○, 2 μM CSA-13; □, 10 μM CSA-13; ●, 30 μM CSA-13. (G to K) Chemiluminescence of *Pseudomonas aeruginosa* Xen5 after the addition of bacteria to the apical interface of polarized A549 cells grown for 1 week on 3-μm-pore inserts, with (right) or without (left) the presence of butyric acid (BA). One hour after inoculation of bacteria, cells were treated with CSA-13 or LL-37 peptide. After the addition of antibacterial molecules, chemiluminescence was evaluated at different time points, i.e., 1 h (G), 2 h (H), or 8 h (I), using a Fuji Film LAS-300 system. Quantitative (densitometric) analysis of chemiluminescence intensity at the epithelial surface of cells growing without (J) or with (K) butyric acid also was performed. A.U., arbitrary units. (L) Decreasing release of IL-8 from A549 lung epithelial cell monolayers growing without or with butyric acid (4 mM) and subjected to LPS (25 ng/ml) activation in the presence of CSA-13 or LL-37 peptide. Error bars, standard deviations ($n = 3$ to 6). *, statistically significant ($P < 0.05$), compared to control group/time zero.

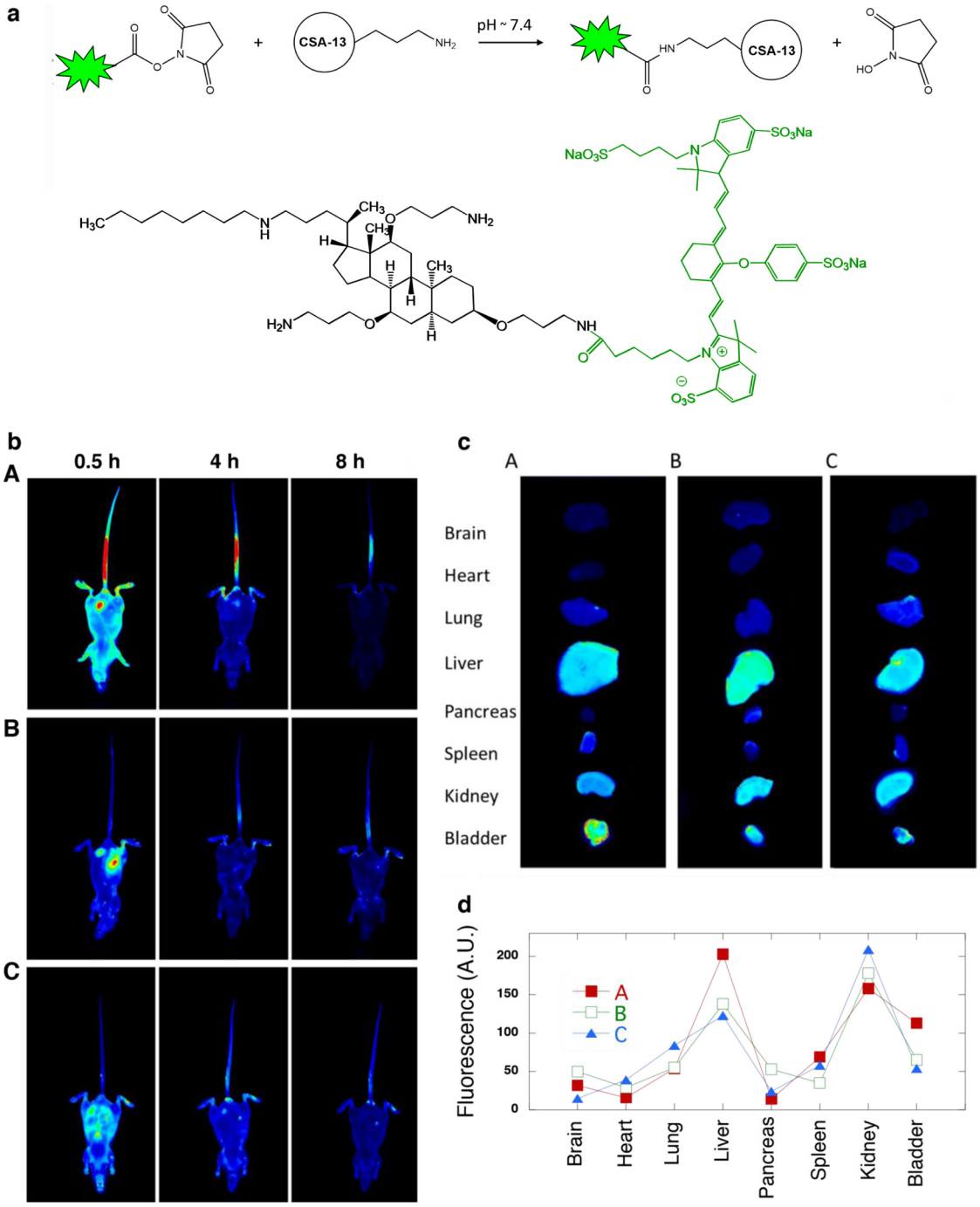

FIG 2 (a) Schematic representation of CSA-13 labeling with IRDye 800CW. The product was obtained through reaction of the NHS ester group of IRDye 800CW with the primary amine group of CSA-13. NHS ester-activated cross-linkers and labeling compounds react with primary amines under physiological conditions (pH 7.4) to yield stable amide bonds. The reaction releases *N*-hydroxysuccinimide (NHS). (b) Visualization of ceragenin biodistribution in whole mice using *in vivo* imaging, showing the intensity of CSA-13–IRDye 800CW distribution after intravenous (A) or intraperitoneal (B and C) administration, in healthy mice (A and B) and mice infected with the PAO1 strain (C). Data were collected after 0.5, 4, and 8 h. (c) Distribution of CSA-13–IRDye 800CW in selected organs sectioned from mice after intravenous (A) or intraperitoneal (B and C) administration, in healthy mice (B) and infected mice (C). (d) Densitometric analysis of organ fluorescence intensity. A.U., arbitrary units. Panels b to d include data from one representative experiment conducted with 5 replicates.

infected with *P. aeruginosa* PAO1 and treated 2 h after intraperitoneal (i.p.) injection of bacteria with an i.p. injection of CSA-13–IRDye 800CW (5 μg/g) or sterile saline solution (control) were euthanized after 8 h for collection of peritoneal fluid samples. Figure 3D shows that CSA-13–IRDye 800CW was effective in significantly reducing bacterial outgrowth (CFU) from peritoneal fluid samples collected from infected animals that had received i.p. injections of CSA-13–IRDye 800CW. Analysis of total white

TABLE 1 Pharmacokinetic parameters assessed for ceragenin CSA-13

Pharmacokinetic parameter[a]	CSA-13 result
C_{max} (μg/ml)	5
T_{max} (h)	0.5
$t_{1/2}$ (h)	2.95
AUC_{total} (μg/ml · h)	20.46
AUC/MIC ratio	6.66
MRT (h)	1.7
CL (ml/h)	4.88
Protein binding (%)	99

[a] C_{max}, maximum plasma concentration; T_{max}, time to reach C_{max}; $t_{1/2}$, biological half-life; AUC_{total}, total area under the concentration-time curve; MRT, mean residence time; CL, clearance.

blood cells (WBCs) indicates systemic inflammatory responses to infections. Figure 3E shows that, in our experimental setting, 3-fold increases in total amounts of WBCs in infected mice occurred 10 h postinfection. However, an expected decrease in total WBC amounts in treated mice versus untreated mice was not observed. No statistically significant difference in the values of the square root of the spleen weight/total body weight ratio for control, infected, and infected/CSA-13–IRDye 800CW-treated animals was observed (Fig. 3F).

DISCUSSION

CSA-13 is a nonpeptide bactericidal molecule with activity against a broad spectrum of Gram-negative and Gram-positive bacteria, particularly clinically relevant pathogens such as *P. aeruginosa* and methicillin-resistant *Staphylococcus aureus* (MRSA) (4, 31). Additionally, this low-molecular-mass compound has potent activity against bacterial biofilms (32, 33). Some previous studies undertook evaluations of CSA-13 activity using *in vitro* systems and different experimental settings dedicated to evaluation of activity against resistant strains (31, 34), in different body fluids (32), in the presence of different polyelectrolytes (35, 36), or using drug release systems and antimicrobial coating (32, 37, 38). However, only a few studies have evaluated the activity of CSA-13 in cell cultures or animal models (13, 39, 40). The *in vivo* activity of CSA-13 likely depends on environmental factors at the infection site, host immune responses, and the type of pathogen causing infection. Compared with controls, CSA-13 did not prevent pin track infection at a percutaneous tibial pin site in a sheep model, suggesting that maintaining skin attachment at the implant surface of osseointegrated implants is essential as a primary barrier to infection (39). Lack of CSA-13 effects at a percutaneous tibial pin site in a sheep model also underlines the importance of host defense mechanisms, which might synergistically support the effectiveness of exogenous antibacterial agents. The need for higher concentrations of CSA-13 to eliminate most of the bacteria at the surface of lung epithelial cells covered by a layer of mucin, compared to the concentrations able to eliminate bacteria in the abdominal cavity, likely results from local environmental differences in the models, since they involved the same pathogen. This possibility supports the observed increase in CSA-13 effects in cell cultures treated with butyric acid, which increases the production of LL-37.

Since bacteria are able to develop resistance to most known classes of natural and synthetic antibiotics, methods to develop new antibiotics or to improve the efficacy of established antibiotics are of great interest. Susceptibility data demonstrated that CSA-13 has an MIC_{50}/minimum bactericidal activity at which 50% of strains tested are killed (MBC_{50}) ratio of 1, suggesting bactericidal activity. This was confirmed by time-kill analysis, which demonstrated that CSA-13 has potent bactericidal activity even at a concentration 0.5 times the MIC (4). Our data confirm previously reported strong bactericidal activity and demonstrate the ability to eliminate bacteria in the abdominal cavity. The *in vivo* bactericidal activity of CSA-13 might be strongly supported by additive and/or synergistic effects of host antibacterial molecules that function as part of a nonspecific mechanism to prevent infection. Since the mechanism of action of CSA-13 has not been fully elucidated, its additive activity might occur through different mechanisms, including strain-specific autolysis promoted by CSA-13 in pneumococcal bacteria due to triggering of the major *Streptococcus pneumoniae* autolysin, LytA (an *N*-acetylmuramoyl-L-alanine amidase) (11), and membrane-permeabilizing capabilities (13).

It is worth noting that the toxicity of CSA-13 has been determined to be low, and the minimum dose required for the desired beneficial effect of CSA-13 (the *in vitro* effective dose) was determined to be 0.5 μg/ml (40). It was recently found that the capacity of CSA-13 to damage host cells could be modulated by Pluronic F-127. This nonionic surfactant was able to decrease the toxicity of CSA-13 toward eukaryotic cells without completely protecting them from mitochondrial damage at high concentrations of the drug (41). Decreased CSA-13 toxicity toward eukaryotic cells in the presence of Pluronic F-127 did not affect its killing activity against bacteria (32). The addition of CSA-13 to fully differentiated cultures of epithelial cells producing mucin (Fig. 1), at a concentration of 30 μg/ml (causing release of about 8% of LDH from confluent cultures of gastric adenocarcinoma cells [3]), does not result in morphological changes of lung epithelial cells. Such an effect suggests that the toxic effects of CSA-13 might decrease when it exerts its antibacterial action in a biopolymer network such as a solution of mucin (35, 42).

Evaluation of ceragenin biodistribution using visualization of CSA-13 labeled with a fluorescent probe, i.e., CSA-13–IRDye 800CW, indicates that its pharmacokinetic features are comparable to those of classic antibiotics (43). According to our findings, CSA-13 shows similarity to fluoroquinolones. In agreement with a study performed by Fahmy and Abu-Gharbieh (44), the elimination half-life of the ceragenin is comparable to the time estimated for ciprofloxacin after compartmental analysis of data obtained in rabbits, which was determined to be within the range of 2.99 to 4.32 h. However, the protein binding analysis revealed the greatest similarity with active steroid compounds, which are structurally related to CSA-13. After intraperitoneal administration, most of the CSA-13–IRDye 800CW was distributed to the liver and kidneys. Strong signals recorded from those organs might reflect the high levels of blood perfusion characterizing the liver and kidneys. However, high levels of fluorescence were not observed in the brain, where the level of blood perfusion is also very high (45, 46). A similar finding was noted by Fischman et al., using noninvasive positron emission tomography (PET) and ^{18}F-labeled fleroxacin to determine the tissue pharmacokinetics of this drug (47). The detected signals might partially represent the fluorescence from molecules used to label CSA-13, as formed after CSA-13–IRDye 800CW hydrolysis. Detected fluorescence, indicating accumulation of CSA-13–IRDye 800CW, in the bladder after intravenous

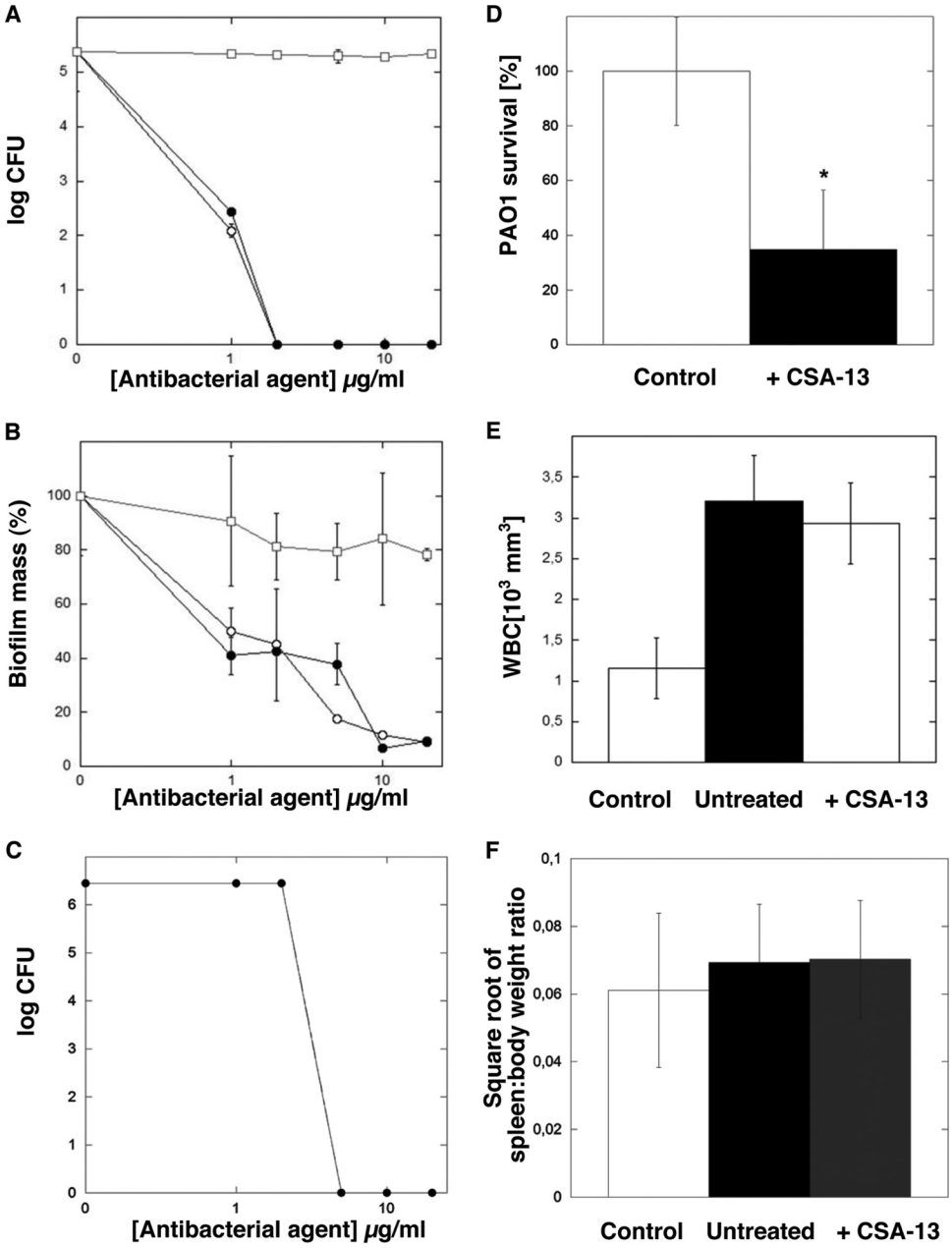

FIG 3 (A and B) Bactericidal activities of CSA-13 (○), CSA-13–IRDye 800CW (●), and IRDye 800CW (□) against planktonic (A) and biofilm-forming (B) *P. aeruginosa* PAO1. Results represent means ± SDs from three experiments. (C and D) CSA-13–IRDye 800CW activities in abdominal fluid (C) and *in vivo* in mice that received CSA-13–IRDye 800CW at a concentration of 5 μg/g (D). Results represent means ± SDs ($n = 5$). *, statistically significant ($P \leq 0.05$), compared to untreated control. (E) Total amounts of WBCs in the blood of healthy mice (control), infected mice (untreated), and infected mice treated with CSA-13–IRDye 800CW after PAO1 challenge. Results represent means ± SDs ($n = 5$). (F) Square root of the spleen weight/total body weight ratio for healthy, CSA-13–IRDye 800CW-treated, and untreated mice 8 h after PAO1 injection. Results represent means ± SDs ($n = 5$).

injection could be attributed to enhanced renal elimination of these molecules, suggesting the dominant role of the bladder in protecting against CSA-13–IRDye 800CW accumulation. However, further studies to evaluate CSA-13 nephrotoxicity are needed. Our data indicate that fluorescence imaging of drug biodistribution could be an alternative method for visualization of drug localization and, after reconstruction, calculation of pharmacological parameters. Recent reports revealed that fluorescence-mediated tomography has many advantages over other techniques, because of the low cost, ease of use, and absence of radioactivity (48). The possibility of overcoming these limitations emphasizes the complex character of these imaging techniques (49). However, other techniques also could be applied for whole-animal map reconstruction (50).

Rapid dose-dependent interactions between bacteria and CSA-13 labeled with a fluorescent probe, boron-dipyrromethene (BODIPY)-succinimidyl ester (CSA-119), were recently reported (51). That study emphasizes that the hydrophobic character of

BODIPY-succinimidyl ester likely contributes to the interactions of CSA-119 with bacteria (51). Similar to the reported properties of CSA-119 resulting from the presence of attached dye, increased affinity of the ceragenin tagged with IRDye 800CW for bacterial cells may partially explain differences in the distribution of CSA-13–IRDye 800CW in the abdominal cavities of healthy versus infected mice. The bactericidal activity of CSA-13 did not significantly change after functionalization with IRDye 800CW. In agreement with our study, Saar-Dover et al. indicated that CAPs labeled with diazole dye at their N termini possessed the net charge of the unlabeled peptides minus one, while their antimicrobial activity was unchanged (52). That study confirmed that, after functionalization with fluorescent groups, cationic antimicrobial peptides and their synthetic analogs retained their activities and affinities for the plasma membranes of bacteria.

ACKNOWLEDGMENTS

This work was financially supported by the National Science Centre of Poland (grant UMO-2012/07/B/NZ6/03504 to R.B.).

In 2013, R.B. and P.A.J. were involved in a sponsored research agreement with Genentech, in a project directed at evaluating the effects of polyaspartate and gelsolin on Pulmozyme activity but not otherwise related to the present study. None of the research reported in this paper was supported by any corporate entity.

REFERENCES

1. **Savage PB, Li C.** 2000. Cholic acid derivatives: novel antimicrobials. Expert Opin Investig Drugs **9:**263–272. http://dx.doi.org/10.1517/13543784.9.2.263.
2. **Savage PB, Li C, Taotafa U, Ding B, Guan Q.** 2002. Antibacterial properties of cationic steroid antibiotics. FEMS Microbiol Lett **217:**1–7. http://dx.doi.org/10.1111/j.1574-6968.2002.tb11448.x.
3. **Leszczynska K, Namiot A, Fein DE, Wen Q, Namiot Z, Savage PB, Diamond S, Janmey PA, Bucki R.** 2009. Bactericidal activities of the cationic steroid CSA-13 and the cathelicidin peptide LL-37 against *Helicobacter pylori* in simulated gastric juice. BMC Microbiol **9:**187. http://dx.doi.org/10.1186/1471-2180-9-187.
4. **Chin JN, Rybak MJ, Cheung CM, Savage PB.** 2007. Antimicrobial activities of ceragenins against clinical isolates of resistant *Staphylococcus aureus*. Antimicrob Agents Chemother **51:**1268–1273. http://dx.doi.org/10.1128/AAC.01325-06.
5. **Howell MD, Streib JE, Kim BE, Lesley LJ, Dunlap AP, Geng D, Feng Y, Savage PB, Leung DY.** 2009. Ceragenins: a class of antiviral compounds to treat orthopox infections. J Invest Dermatol **129:**2668–2675. http://dx.doi.org/10.1038/jid.2009.120.
6. **Lara D, Feng Y, Bader J, Savage P, Maldonado R.** 2010. Anti-trypanosomatid activity of ceragenins. J Parasitol **96:**638–642. http://dx.doi.org/10.1645/GE-2329.1.
7. **Leszczynska K, Namiot D, Byfield FJ, Cruz K, Zendzian-Piotrowska M, Fein DE, Savage PB, Diamond S, McCulloch CA, Janmey PA, Bucki R.** 2013. Antibacterial activity of the human host defence peptide LL-37 and selected synthetic cationic lipids against bacteria associated with oral and upper respiratory tract infections. J Antimicrob Chemother **68:**610–618. http://dx.doi.org/10.1093/jac/dks434.
8. **Sevgi M, Toklu A, Vecchio D, Hamblin MR.** 2013. Topical antimicrobials for burn infections: an update. Recent Pat Antiinfect Drug Discov **8:**161–197. http://dx.doi.org/10.2174/15748898113089990001.
9. **Sinclair KD, Pham TX, Williams DL, Farnsworth RW, Loc-Carrillo CM, Bloebaum RD.** 2013. Model development for determining the efficacy of a combination coating for the prevention of perioperative device related infections: a pilot study. J Biomed Mater Res B Appl Biomater **101:**1143–1153. http://dx.doi.org/10.1002/jbm.b.32924.
10. **Pollard JE, Snarr J, Chaudhary V, Jennings JD, Shaw H, Christiansen B, Wright J, Jia W, Bishop RE, Savage PB.** 2012. In vitro evaluation of the potential for resistance development to ceragenin CSA-13. J Antimicrob Chemother **67:**2665–2672. http://dx.doi.org/10.1093/jac/dks276.
11. **Moscoso M, Esteban-Torres M, Menendez M, Garcia E.** 2014. In vitro bactericidal and bacteriolytic activity of ceragenin CSA-13 against planktonic cultures and biofilms of *Streptococcus pneumoniae* and other pathogenic streptococci. PLoS One **9:**e101037. http://dx.doi.org/10.1371/journal.pone.0101037.
12. **Nagant C, Pitts B, Stewart PS, Feng Y, Savage PB, Dehaye JP.** 2013. Study of the effect of antimicrobial peptide mimic, CSA-13, on an established biofilm formed by *Pseudomonas aeruginosa*. Microbiologyopen **2:**318–325. http://dx.doi.org/10.1002/mbo3.77.
13. **Kuroda K, Fukuda T, Okumura K, Yoneyama H, Isogai H, Savage PB, Isogai E.** 2013. Ceragenin CSA-13 induces cell cycle arrest and antiproliferative effects in wild-type and p53 null mutant HCT116 colon cancer cells. Anticancer Drugs **24:**826–834. http://dx.doi.org/10.1097/CAD.0b013e3283634dd0.
14. **Epand RF, Savage PB, Epand RM.** 2007. Bacterial lipid composition and the antimicrobial efficacy of cationic steroid compounds (ceragenins). Biochim Biophys Acta **1768:**2500–2509. http://dx.doi.org/10.1016/j.bbamem.2007.05.023.
15. **Epand RF, Pollard JE, Wright JO, Savage PB, Epand RM.** 2010. Depolarization, bacterial membrane composition, and the antimicrobial action of ceragenins. Antimicrob Agents Chemother **54:**3708–3713. http://dx.doi.org/10.1128/AAC.00380-10.
16. **Evans SE, Xu Y, Tuvim MJ, Dickey BF.** 2010. Inducible innate resistance of lung epithelium to infection. Annu Rev Physiol **72:**413–435. http://dx.doi.org/10.1146/annurev-physiol-021909-135909.
17. **McCray PB, Jr, Bentley L.** 1997. Human airway epithelia express a beta-defensin. Am J Respir Cell Mol Biol **16:**343–349. http://dx.doi.org/10.1165/ajrcmb.16.3.9070620.
18. **Goldman MJ, Anderson GM, Stolzenberg ED, Kari UP, Zasloff M, Wilson JM.** 1997. Human β-defensin-1 is a salt-sensitive antibiotic in lung that is inactivated in cystic fibrosis. Cell **88:**553–560. http://dx.doi.org/10.1016/S0092-8674(00)81895-4.
19. **Chen CI, Schaller-Bals S, Paul KP, Wahn U, Bals R.** 2004. β-Defensins and LL-37 in bronchoalveolar lavage fluid of patients with cystic fibrosis. J Cyst Fibros **3:**45–50. http://dx.doi.org/10.1016/j.jcf.2003.12.008.
20. **Bucki R, Leszczynska K, Namiot A, Sokolowski W.** 2010. Cathelicidin LL-37: a multitask antimicrobial peptide. Arch Immunol Ther Exp (Warsz) **58:**15–25. http://dx.doi.org/10.1007/s00005-009-0057-2.
21. **Karlsson J, Carlsson G, Larne O, Andersson M, Putsep K.** 2008. Vitamin D_3 induces pro-LL-37 expression in myeloid precursors from patients with severe congenital neutropenia. J Leukoc Biol **84:**1279–1286. http://dx.doi.org/10.1189/jlb.0607437.
22. **Gombart AF, O'Kelly J, Saito T, Koeffler HP.** 2007. Regulation of the CAMP gene by $1,25(OH)_2D_3$ in various tissues. J Steroid Biochem Mol Biol **103:**552–557. http://dx.doi.org/10.1016/j.jsbmb.2006.12.095.
23. **Maiti S, Patro S, Purohit S, Jain S, Senapati S, Dey N.** 2014. Effective control of *Salmonella* infections by employing combinations of recombinant antimicrobial human β-defensins hBD-1 and hBD-2. Antimicrob Agents Chemother **58:**6896–6903. http://dx.doi.org/10.1128/AAC.03628-14.
24. **Cavanagh JP, Granslo HN, Fredheim EA, Christophersen L, Jensen PO, Thomsen K, Van Gennip M, Klingenberg C, Flaegstad T, Moser C.** 2013. Efficacy of a synthetic antimicrobial peptidomimetic versus vancomycin in a *Staphylococcus epidermidis* device-related murine peritonitis model. J Antimicrob Chemother **68:**2106–2110. http://dx.doi.org/10.1093/jac/dkt161.
25. **Hase K, Eckmann L, Leopard JD, Varki N, Kagnoff MF.** 2002. Cell differentiation is a key determinant of cathelicidin LL-37/human cationic antimicrobial protein 18 expression by human colon epithelium. Infect Immun **70:**953–963. http://dx.doi.org/10.1128/IAI.70.2.953-963.2002.
26. **Schwab M, Reynders V, Shastri Y, Loitsch S, Stein J, Schroder O.** 2007. Role of nuclear hormone receptors in butyrate-mediated up-regulation of the antimicrobial peptide cathelicidin in epithelial colorectal cells. Mol Immunol **44:**2107–2114. http://dx.doi.org/10.1016/j.molimm.2006.09.016.
27. **Nanda JS, Lorsch JR.** 2014. Labeling a protein with fluorophores using NHS ester derivitization. Methods Enzymol **536:**87–94. http://dx.doi.org/10.1016/B978-0-12-420070-8.00008-8.
28. **Gootz TD, Subashi TA, Lindner DL.** 1988. Simple spectrophotometric assay for measuring protein binding of penem antibiotics to human serum. Antimicrob Agents Chemother **32:**159–163. http://dx.doi.org/10.1128/AAC.32.2.159.
29. **Plotkowski MC, de Bentzmann S, Pereira SH, Zahm JM, Bajolet-Laudinat O, Roger P, Puchelle E.** 1999. *Pseudomonas aeruginosa* internalization by human epithelial respiratory cells depends on cell differen-

tiation, polarity, and junctional complex integrity. Am J Respir Cell Mol Biol **20:**880–890. http://dx.doi.org/10.1165/ajrcmb.20.5.3408.
30. **Lee A, Chow D, Haus B, Tseng W, Evans D, Fleiszig S, Chandy G, Machen T.** 1999. Airway epithelial tight junctions and binding and cytotoxicity of *Pseudomonas aeruginosa*. Am J Physiol **277:**L204–L217.
31. **Chin JN, Jones RN, Sader HS, Savage PB, Rybak MJ.** 2008. Potential synergy activity of the novel ceragenin, CSA-13, against clinical isolates of *Pseudomonas aeruginosa*, including multidrug-resistant *P. aeruginosa*. J Antimicrob Chemother **61:**365–370.
32. **Leszczynska K, Namiot A, Cruz K, Byfield FJ, Won E, Mendez G, Sokolowski W, Savage PB, Bucki R, Janmey PA.** 2011. Potential of ceragenin CSA-13 and its mixture with pluronic F-127 as treatment of topical bacterial infections. J Appl Microbiol **110:**229–238. http://dx.doi.org/10.1111/j.1365-2672.2010.04874.x.
33. **Surel U, Niemirowicz K, Marzec M, Savage P, Bucki R.** 2014. Ceragenins: a new weapon to fight multidrug resistant bacterial infections. Studia Med **30:**207–213.
34. **Bozkurt-Guzel C, Savage PB, Akcali A, Ozbek-Celik B.** 2014. Potential synergy activity of the novel ceragenin, CSA-13, against carbapenem-resistant *Acinetobacter baumannii* strains isolated from bacteremia patients. Biomed Res Int **2014:**710273.
35. **Bucki R, Namiot DB, Namiot Z, Savage PB, Janmey PA.** 2008. Salivary mucins inhibit antibacterial activity of the cathelicidin-derived LL-37 peptide but not the cationic steroid CSA-13. J Antimicrob Chemother **62:**329–335. http://dx.doi.org/10.1093/jac/dkn176.
36. **Bucki R, Sostarecz AG, Byfield FJ, Savage PB, Janmey PA.** 2007. Resistance of the antibacterial agent ceragenin CSA-13 to inactivation by DNA or F-actin and its activity in cystic fibrosis sputum. J Antimicrob Chemother **60:**535–545. http://dx.doi.org/10.1093/jac/dkm218.
37. **Sinclair KD, Pham TX, Farnsworth RW, Williams DL, Loc-Carrillo C, Horne LA, Ingebretsen SH, Bloebaum RD.** 2012. Development of a broad spectrum polymer-released antimicrobial coating for the prevention of resistant strain bacterial infections. J Biomed Mater Res A **100:**2732–2738. http://dx.doi.org/10.1002/jbm.a.34209.
38. **Williams DL, Sinclair KD, Jeyapalina S, Bloebaum RD.** 2013. Characterization of a novel active release coating to prevent biofilm implant-related infections. J Biomed Mater Res B Appl Biomater **101:**1078–1089. http://dx.doi.org/10.1002/jbm.b.32918.
39. **Perry EL, Beck JP, Williams DL, Bloebaum RD.** 2010. Assessing periimplant tissue infection prevention in a percutaneous model. J Biomed Mater Res B Appl Biomater **92:**397–408.
40. **Saha S, Savage PB, Bal M.** 2008. Enhancement of the efficacy of erythromycin in multiple antibiotic-resistant Gram-negative bacterial pathogens. J Appl Microbiol **105:**822–828. http://dx.doi.org/10.1111/j.1365-2672.2008.03820.x.
41. **Nagant C, Savage PB, Dehaye JP.** 2012. Effect of pluronic acid F-127 on the toxicity towards eukaryotic cells of CSA-13, a cationic steroid analogue of antimicrobial peptides. J Appl Microbiol **112:**1173–1183. http://dx.doi.org/10.1111/j.1365-2672.2012.05297.x.
42. **Bucki R, Pastore JJ, Randhawa P, Vegners R, Weiner DJ, Janmey PA.** 2004. Antibacterial activities of rhodamine B-conjugated gelsolin-derived peptides compared to those of the antimicrobial peptides cathelicidin LL37, magainin II, and melittin. Antimicrob Agents Chemother **48:**1526–1533. http://dx.doi.org/10.1128/AAC.48.5.1526-1533.2004.
43. **Guillard T, Cambau E, Chau F, Massias L, de Champs C, Fantin B.** 2013. Ciprofloxacin treatment failure in a murine model of pyelonephritis due to an AAC(6′)-Ib-cr-producing *Escherichia coli* strain susceptible to ciprofloxacin in vitro. Antimicrob Agents Chemother **57:**5830–5835. http://dx.doi.org/10.1128/AAC.01489-13.
44. **Fahmy S, Abu-Gharbieh E.** 2014. In vitro dissolution and in vivo bioavailability of six brands of ciprofloxacin tablets administered in rabbits and their pharmacokinetic modeling. Biomed Res Int **2014:**590848.
45. **Stott WT, Dryzga MD, Ramsey JC.** 1983. Blood-flow distribution in the mouse. J Appl Toxicol **3:**310–312. http://dx.doi.org/10.1002/jat.2550030607.
46. **Krishnan K, Crouse LC, Bazar MA, Major MA, Reddy G.** 2009. Physiologically based pharmacokinetic modeling of cyclotrimethylenetrinitramine in male rats. J Appl Toxicol **29:**629–637. http://dx.doi.org/10.1002/jat.1455.
47. **Fischman AJ, Livni E, Babich J, Alpert NM, Liu YY, Thom E, Cleeland R, Prosser BL, Correia JA, Strauss HW.** 1993. Pharmacokinetics of [^{18}F]fleroxacin in healthy human subjects studied by using positron emission tomography. Antimicrob Agents Chemother **37:**2144–2152. http://dx.doi.org/10.1128/AAC.37.10.2144.
48. **Gremse F, Theek B, Kunjachan S, Lederle W, Pardo A, Barth S, Lammers T, Naumann U, Kiessling F.** 2014. Absorption reconstruction improves biodistribution assessment of fluorescent nanoprobes using hybrid fluorescence-mediated tomography. Theranostics **4:**960–971. http://dx.doi.org/10.7150/thno.9293.
49. **Baker M.** 2010. Whole-animal imaging: the whole picture. Nature **463:**977–980. http://dx.doi.org/10.1038/463977a.
50. **Ntziachristos V, Ripoll J, Wang LV, Weissleder R.** 2005. Looking and listening to light: the evolution of whole-body photonic imaging. Nat Biotechnol **23:**313–320. http://dx.doi.org/10.1038/nbt1074.
51. **Nagant C, Feng Y, Lucas B, Braeckmans K, Savage P, Dehaye JP.** 2011. Effect of a low concentration of a cationic steroid antibiotic (CSA-13) on the formation of a biofilm by *Pseudomonas aeruginosa*. J Appl Microbiol **111:**763–772. http://dx.doi.org/10.1111/j.1365-2672.2011.05085.x.
52. **Saar-Dover R, Bitler A, Nezer R, Shmuel-Galia L, Firon A, Shimoni E, Trieu-Cuot P, Shai Y.** 2012. D-Alanylation of lipoteichoic acids confers resistance to cationic peptides in group B streptococcus by increasing the cell wall density. PLoS Pathog **8:**e1002891. http://dx.doi.org/10.1371/journal.ppat.1002891.